V47

Temperature dependence of molar heat of copper

Christopher Breitfeld
christopher.breitfeld@tu-dortmund.de

Henry Krämerkämper
henry.kraemerkaemper@tu-dortmund.de

Conducted: 22. January 2024 Submission: February 15, 2024

TU Dortmund – Fakultät Physik

Contents

1 Aims of the Experiment **3**

2 Theory **3**
2.1 Classical and Quantum Mechanical Description of Temperature 4
2.2 Einstein Model 4
2.3 Debye Model 4

3 Experimental Setup and Measurements **5**

4 Analysis **7**
4.1 Determination of C_p and C_V 7
4.2 Determination of the Debye Temperature 9
4.3 Results 13

5 Discussion **13**

References **13**

1 Aims of the Experiment

The primary aim of the experiment is to determine the Debye temperature θ_D of copper. This will be achieved by measuring the isobaric specific heat capacity C_p of the material. The Debye temperature is a fundamental characteristic of a crystalline solid, representing the temperature above which all modes of lattice vibration are excited.

2 Theory

The heat capacity of a solid is defined as the amount of heat ΔQ that must be added to the solid to raise its temperature by ΔT. The heat capacity can be expressed as the limit for infinitesimal temperature changes

$$C = \lim_{\Delta T \to 0} \frac{\Delta Q}{\Delta T}. \tag{1}$$

The specific heat capacity refers to the heat capacity per unit mass, volume, or amount of substance of the sample. It is distinguished by the following definitions

$$c^n = \frac{C}{n} \qquad c^V = \frac{C}{V} \qquad c^m = \frac{C}{m}$$

where n is the molar amount, V is the volume, and m is the mass of the substance, respectively.

According to the first law of thermodynamics

$$\mathrm{d}Q = \mathrm{d}U + p\mathrm{d}V \tag{2}$$

two different heat capacities can be defined. Under the assumption of constant volume ($\mathrm{d}V = 0$), equation (1) yields

$$C_V = \left(\frac{\partial Q}{\partial T}\right)_{V=const.} = \left(\frac{\partial U}{\partial T}\right)_V. \tag{3}$$

Expressing the inner energy as a function of pressure p and temperature T equation (2) results in

$$\mathrm{d}Q = \left(\frac{\partial U}{\partial T}\right)_p \mathrm{d}T + \left(\frac{\partial U}{\partial p}\right)_T \mathrm{d}p + p\left(\frac{\partial V}{\partial T}\right)_p \mathrm{d}T + p\left(\frac{\partial V}{\partial p}\right)_T \mathrm{d}p.$$

For an isobaric process ($\mathrm{d}p = 0$), the heat capacity at constant pressure is given by

$$C_p = \left(\frac{\partial Q}{\partial T}\right)_{p=const.} = \left(\frac{\partial U}{\partial T}\right)_p + p\left(\frac{\partial V}{\partial T}\right)_p. \tag{4}$$

The difference between the heat capacities at constant pressure and volume is determined to be

$$C_p - C_V = 9\alpha^2 \kappa V_0 T \tag{5}$$

where α is the coefficient of thermal expansion, and κ is the bulk modulus.

While C_V measures the increase in inner energy per degree of temperature increase, C_p also includes the energy used for the work done due to expansion. As a result, $C_p - C_V > 0$. Since gases expand significantly more than solids with temperature changes, the difference between C_p and C_V is much larger for gases compared to solids.

2.1 Classical and Quantum Mechanical Description of Temperature

The oscillations of atoms inside a solid can be approximated by harmonic oscillations.

In a classical system, a harmonic oscillator has a continuous energy spectrum. Each mode contributes an average energy of $\frac{1}{2}k_BT$. In a three-dimensional system with N atoms, there are six degrees of freedom — three spatial and three for momentum. This leads to a total energy of $3Nk_BT$ and, accordingly, a heat capacity of

$$C_V^{\mathrm{D}} = 3Nk_B. \tag{6}$$

This is the high-temperature approximation of heat capacity known as the Dulong-Petit law.

In contrast, a quantum mechanical harmonic oscillator has discrete energy levels given by $\hbar\omega(n+1/2)$. To excite this oscillator, an energy large enough to reach the next level is required, i.e., $k_BT > \hbar\omega$. For $k_BT < \hbar\omega$, no new modes are excited, leading to a reduction in heat capacity as the temperature decreases. This quantum mechanical behavior is key to explaining the deviation from the Dulong-Petit law at low temperatures.

2.2 Einstein Model

The Einstein model assumes $3N$ eigenmodes, each with the same frequency ω_E. This leads to an approximated average inner energy of

$$\langle U\rangle = 3N\hbar\omega_{\mathrm{E}}\left(\frac{1}{2} + \exp\left(\frac{\hbar\omega_{\mathrm{E}}}{k_{\mathrm{B}}T}\right) - 1\right). \tag{7}$$

This yields a heat capacity of

$$C_V^{\mathrm{Einstein}} = 3Nk_{\mathrm{B}}\left(\frac{\theta_{\mathrm{E}}}{T}\right)^2 \frac{\exp\left(\frac{\theta_{\mathrm{E}}}{T}\right)}{\left[\exp\left(\frac{\theta_{\mathrm{E}}}{T}\right)-1\right]^2} = \begin{cases} 3Nk_{\mathrm{B}}\left(\frac{\theta_{\mathrm{E}}}{T}\right)^2 \exp\left(\frac{-\theta_{\mathrm{E}}}{T}\right), & T \ll \theta_{\mathrm{D}} \\ 3Nk_{\mathrm{B}}, & T \gg \theta_{\mathrm{D}} \end{cases} \tag{8}$$

where $\theta_{\mathrm{E}} = \frac{\hbar\omega_{\mathrm{E}}}{k_{\mathrm{B}}}$ is the specific Einstein temperature.

This model predicts the Dulong-Petit law (6) at high temperatures. However, at low temperatures, it fails to account for the experimentally observed T^3 decrease in heat capacity. This limitation can be attributed to the fact that the model only considers optical modes and neglects acoustic modes.

2.3 Debye Model

The Debye model, an improvement over the Einstein model, is particularly effective at low temperatures as it incorporates acoustic modes. Contrary to the Einstein model, which assumes a uniform oscillation frequency for all atoms, the Debye model accounts for a continuous spectrum of vibrations.

In the Debye model, vibrational modes are approximated with a linear dispersion relation for low frequencies, described as $\omega = v_i k$.

The state density function in the Debye model is given by

$$D(\omega) = \frac{Vk^2}{2\pi^2 v} = \frac{V\omega^2}{2\pi^2 v^3}. \tag{9}$$

The heat capacity at constant volume is derived by integrating over all vibrational modes

$$C_V^{\text{Debye}} = 9Nk_{\text{B}}\left(\frac{T}{\theta_{\text{D}}}\right)^3 \int_0^{\frac{\theta_{\text{D}}}{T}} \frac{x^4 \text{e}^x \,\text{d}x}{(\text{e}^x - 1)^2} = \begin{cases} \frac{12\pi^4}{5} Nk_{\text{B}}\left(\frac{T}{\theta_{\text{D}}}\right)^3, & T \ll \theta_{\text{E}} \\ 3Nk_{\text{B}}, & T \gg \theta_{\text{E}} \end{cases} \tag{10}$$

where $x = \hbar\omega/k_{\text{B}}T$, and θ_{D} is the material-specific Debye temperature, defined as

$$\theta_{\text{D}} = \frac{\hbar\omega_{\text{D}}}{k_{\text{B}}} = \frac{\hbar v}{k_{\text{B}}}\left(6\pi^2 \frac{N}{V}\right)^{\frac{1}{3}}. \tag{11}$$

The Debye model accurately predicts the T^3 dependence of heat capacity at low temperatures, consistent with experimental observations. At high temperatures, it aligns with the Dulong-Petit law (6), similar to the Einstein model.

Integrating the state density function (9) from $\omega = 0$ to the Debye frequency ω_D gives

$$\int_0^{\omega_D} D(\omega)\text{d}\omega = 3N \tag{12}$$

resulting in the Debye frequency

$$\omega_D = v_i\left(6\pi^2 \frac{N}{V}\right). \tag{13}$$

The speed of sound v_s can be determined from the speeds v_i for each mode i using

$$\frac{1}{v_s^2} = \frac{1}{3}\sum_{i=1}^{3} \frac{1}{v_i^3}. \tag{14}$$

3 Experimental Setup and Measurements

The experimental setup consists of a cryogenic storage dewar, a type of vacuum flask. Inside this dewar, there is a recipient filled with 342 g of copper. Both the probe and the vessel are heated using an electric heating coil. This setup is schematically illustrated in Figure 1.

Initially, the recipient is evacuated. Subsequently, the dewar is filled with liquid nitrogen to cool the probe down to 80 K. To ensure effective thermal conduction during the cooling process, the recipient is filled with helium. The temperature T is not measured directly but inferred from the resistance R. The temperature can be calculated using the equation

$$T = 0.001\,34R^2 + 2.296R - 243.02 \tag{15}$$

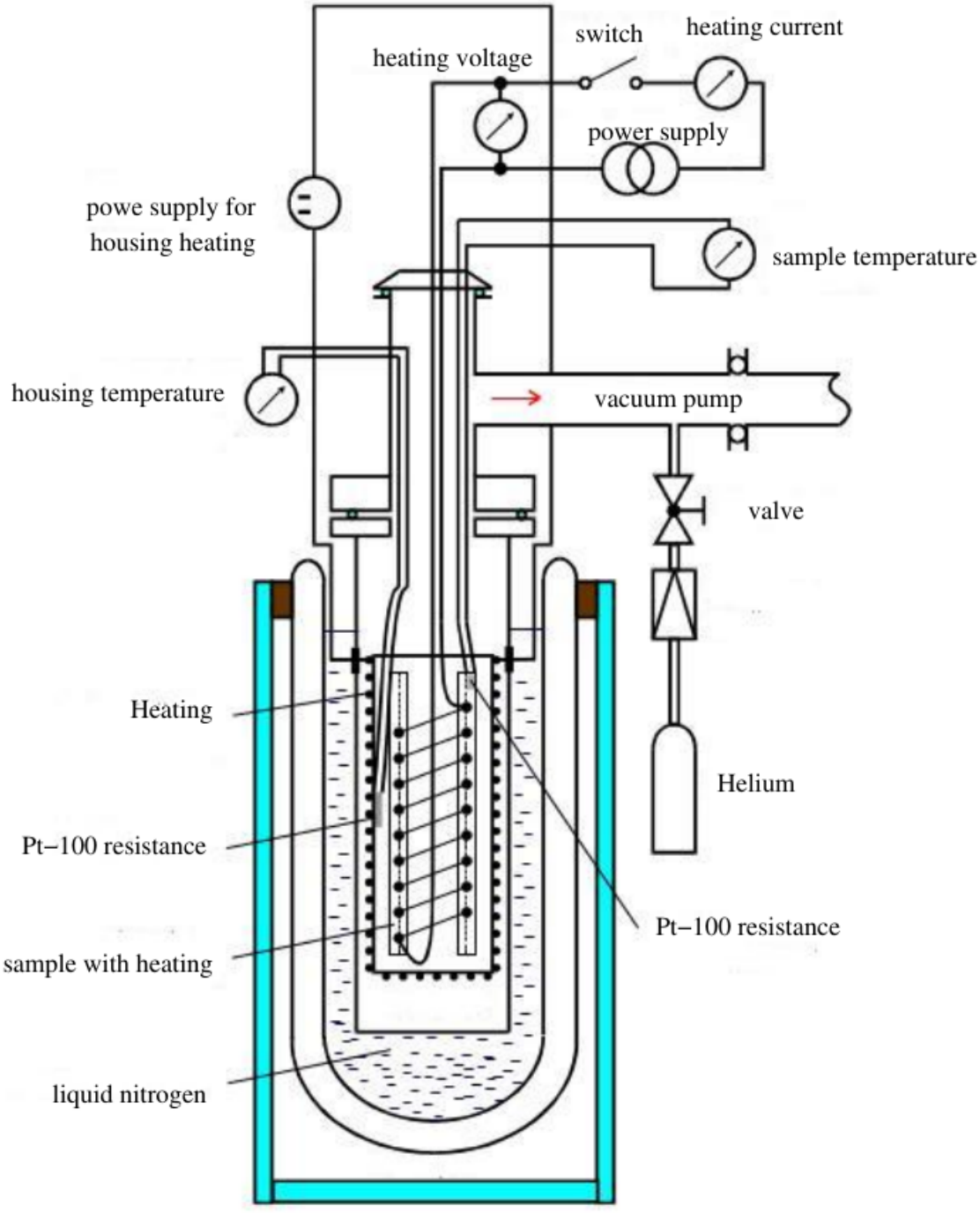

Figure 1: Schematic illustration of the experimental setup. [1]

where the resistance R is measured in Ω, and the temperature is calculated in °C. A temperature of 80 K corresponds to a resistance of approximately 22 Ω.

After cooling, the recipient is evacuated again. The heating coil is set to a constant current of 150 mA, resulting in an increase in resistance. A second coil ensures that the temperatures of the probe and the vessel remain equal.

The current and the resistance of both coils are measured every 2 min. The measurement concludes once the temperature reaches 300 K.

4 Analysis

4.1 Determination of C_p and C_V

The molar heat capacity at constant pressure can be calculated using equation 16.

$$C_p = \frac{U \cdot I \cdot \Delta t \cdot M}{\Delta T \cdot m}. \tag{16}$$

Here, U denotes the heating voltage, I the heating current, Δt the heating time interval, M the molar mass of copper, ΔT the achieved temperature increase and m the mass of the probe. The measured resistances are converted to the corresponding temperatures using Equation 15. The mean of the temperature of the dewar and the outer shell is used throughout the following calculations. The measurement accuracy is estimated to be ± 0.5 for U and I and ± 0.05 min regarding the time measurement. The molar heat capacity at constant volume is computed using 5. The needed physical constants for these calculations are given in Table 1. The calculation of C_V using 5 depends on the

Table 1: Physical constants used.

Constant	Value	Source
m	0.342 kg	[1]
M	0.063 55 kg/mol	[2]
κ	137.8 GPa	[3]
ρ	8.96×10^{-6} kg/mm^3	[3]
v	3570 m/s	[4]

coefficient of thermal expansion α, which is estimated by conducting an interpolation based on the values given in [1]; the interpolating curve consists of cubic spline functions. The results are displayed in Figure 2 and used to calculate C_V.

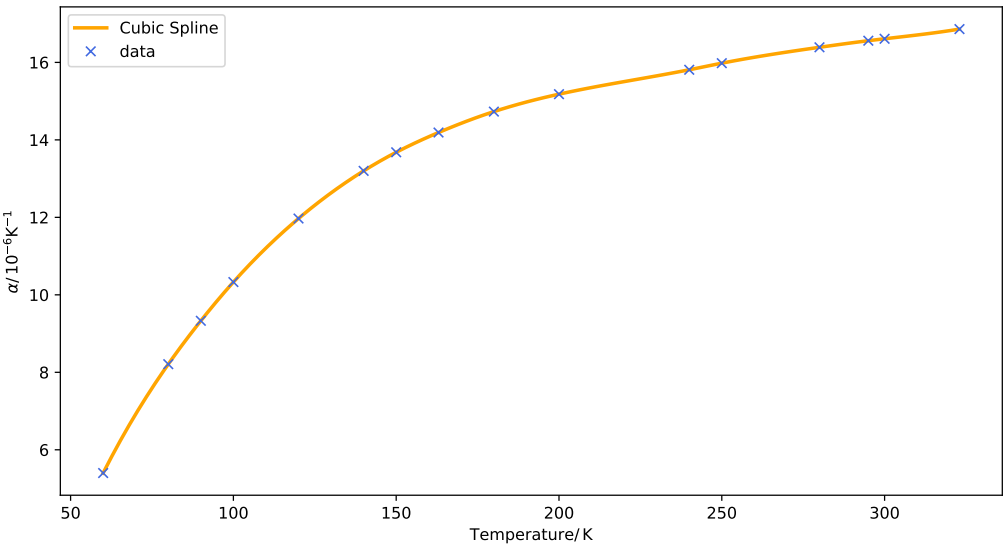

Figure 2: Interpolation of known values of α using cubic splines.

The resulting values for C_p and C_V are plotted against the mean temperature in Figure 3 and given in Table 2 and 3.

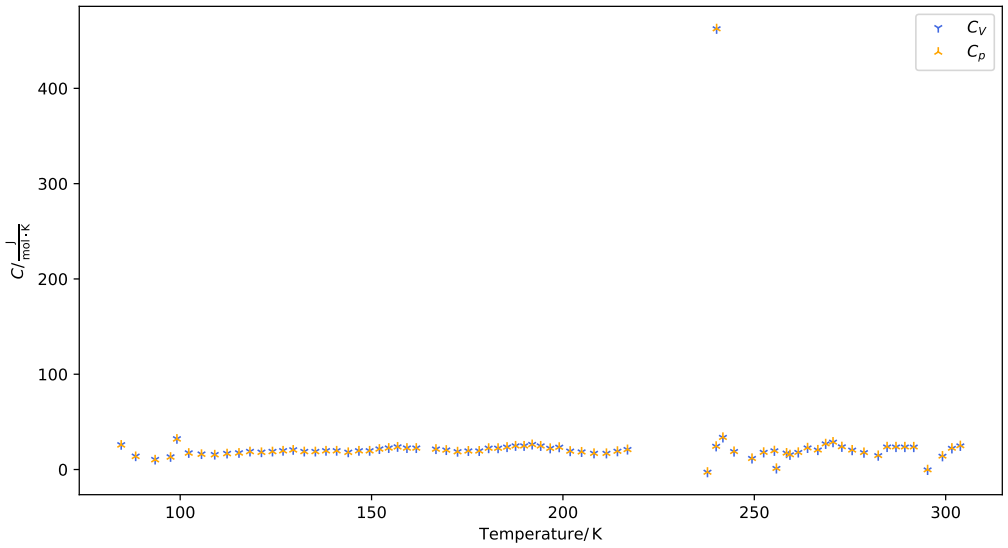

Figure 3: The computed values of C_p and C_V for different temperatures.

Given that the results for C_V and C_p at $T \approx 240\,\mathrm{K}$ deviate by several orders of magnitude, the visualization is performed again without these outlier values to enable a clearer observation of the temperature dependence; the results are displayed in Figure 4.

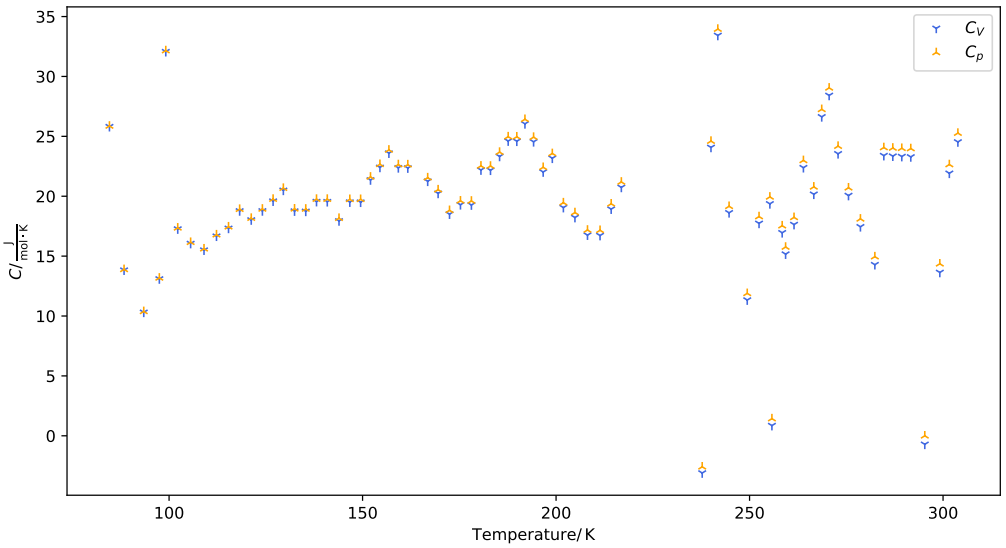

Figure 4: The computed values of C_p and C_V for different temperatures with an outlier removed.

4.2 Determination of the Debye Temperature

To determine the Debye temperature Θ_D, the measured temperatures T are multiplied with the factor $\frac{\Theta_D}{T}$, which is estimated using an interpolation of cubic splines based on the data given in [1]. The resulting interpolation is given in Figure 5.

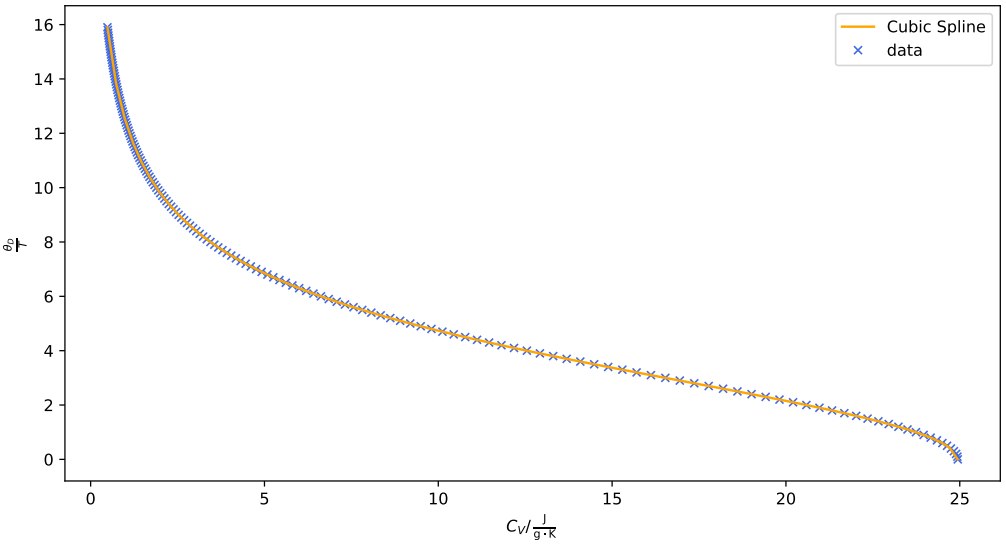

Figure 5: Interpolation of known values of Θ using cubic splines.

The resulting values of Θ_D are given in Table 2 and 3. The Debye temperature can be calculated theoretically using Equation 11. The copper probe used has a volume of

$$V = \frac{m}{\rho} = 3.82 \times 10^{-5}\,\mathrm{m}^3. \tag{17}$$

Here, m denotes the probe mass and ρ is the density. The number of particles N can be calculated using

$$N = \frac{m}{M} \cdot N_A = 3.24 \times 10^{24}\,, \tag{18}$$

with the probes' molar mass M. Utilizing the results from 17 and 18, Equation 11 as well as the speed of sound in copper v, results in a theoretical Debye temperature of

$$\Theta_{D\ \mathrm{Theory}} = 467.14\,\mathrm{K}. \tag{19}$$

Table 2: Measured parameters and corresponding computed results for C_p and C_V (Part 1).

t/min	R_G/Ω	R_P/Ω	I/mA	U/V	T/K	C_p/J/(mol K)	$\alpha/10^{-6}\cdot$K	C_V/J/(mol K)	Θ_D/K
0	23.10	23.70	148.80	15.59	84.59	25.9	8.74	25.8	-9.44×10^4
2	24.50	25.50	149.90	15.70	88.37	13.9	9.16	13.8	323.94
4	27.50	26.80	150.30	15.76	93.45	10.4	9.69	10.3	433.81
6	29.40	28.30	150.70	15.81	97.49	13.2	10.09	13.1	375.85
8	29.50	29.60	151.10	15.86	99.15	32.2	10.25	32.1	-5.41×10^7
10	30.60	31.10	151.40	15.89	102.24	17.4	10.54	17.3	288.79
12	32.20	32.30	151.60	15.93	105.57	16.2	10.83	16.0	329.00
14	33.70	33.70	151.80	15.95	109.03	15.6	11.13	15.5	354.38
16	35.10	35.00	152.00	15.97	112.25	16.8	11.39	16.7	333.24
18	36.40	36.30	152.10	16.00	115.36	17.5	11.63	17.3	324.32
20	37.60	37.50	152.30	16.01	118.23	18.9	11.84	18.8	290.73
22	38.80	38.80	152.40	16.03	121.23	18.2	12.06	18.0	320.37
24	40.00	40.00	152.50	16.05	124.11	18.9	12.25	18.8	305.13
26	41.10	41.20	152.60	16.06	126.88	19.8	12.44	19.6	286.36
28	42.20	42.30	152.70	16.08	129.53	20.7	12.60	20.5	262.35
30	43.40	43.50	152.80	16.09	132.42	18.9	12.78	18.8	326.02
32	44.60	44.70	152.80	16.10	135.32	18.9	12.95	18.7	333.91
34	45.80	45.80	152.90	16.11	138.10	19.8	13.10	19.6	312.98
36	47.00	46.90	153.00	16.12	140.88	19.8	13.25	19.5	319.61
38	48.30	48.10	153.00	16.13	143.91	18.2	13.40	17.9	383.00
40	49.50	49.20	153.10	16.14	146.70	19.7	13.53	19.5	334.06
42	50.60	50.40	153.20	16.15	149.50	19.7	13.66	19.5	340.75
44	51.60	51.50	153.20	16.16	152.05	21.6	13.77	21.4	272.37
46	52.60	52.50	153.20	16.16	154.49	22.7	13.87	22.4	228.96
48	53.40	53.60	153.30	16.17	156.80	23.9	13.96	23.6	166.26
50	54.30	54.70	153.30	16.17	159.24	22.6	14.05	22.4	237.78
52	55.30	55.70	153.30	16.18	161.69	22.6	14.14	22.4	242.36
56	57.50	57.70	153.40	16.19	166.83	21.5	14.32	21.2	303.96
58	58.70	58.70	153.40	16.20	169.52	20.5	14.41	20.2	354.63
60	60.00	59.80	153.50	16.20	172.47	18.8	14.51	18.5	435.41
62	61.20	60.90	153.50	16.20	175.30	19.6	14.60	19.3	408.80
64	62.40	62.00	153.50	16.21	178.13	19.6	14.68	19.3	416.35
66	63.40	63.00	153.60	16.21	180.59	22.5	14.75	22.2	279.90
68	64.40	64.00	153.60	16.22	183.06	22.5	14.81	22.2	284.76
70	65.20	65.10	153.60	16.22	185.40	23.7	14.87	23.3	216.56
72	66.00	66.10	153.60	16.22	187.63	25.0	14.92	24.6	98.30
74	66.80	67.10	153.70	16.22	189.85	25.0	14.97	24.6	101.73
76	67.60	68.00	153.70	16.23	191.96	26.4	15.02	26.0	-4.28×10^5

Table 3: Measured parameters and corresponding computed results for C_p and C_V (Part 2).

t/min	R_G/Ω	R_P/Ω	I/mA	U/V	T/K	C_p/J/(mol K)	$\alpha/10^{-6}\cdot$ K	C_V/J/(mol K)	Θ_D/K
78	68.40	69.00	153.70	16.23	194.19	24.9	15.07	24.5	110.61
80	69.40	70.00	153.70	16.23	196.67	22.4	15.12	22.0	314.70
82	70.40	70.90	153.70	16.23	199.03	23.6	15.16	23.2	243.74
84	71.70	71.90	153.70	16.24	201.89	19.5	15.21	19.1	482.60
86	73.10	72.90	153.80	16.24	204.88	18.6	15.27	18.2	531.34
88	74.70	73.90	153.80	16.24	208.12	17.2	15.32	16.8	613.32
90	76.20	75.00	153.80	16.24	211.37	17.2	15.37	16.7	624.61
92	77.50	76.00	153.80	16.24	214.24	19.4	15.42	18.9	518.97
94	78.50	77.10	153.80	16.24	216.87	21.2	15.46	20.7	425.26
96	78.80	107.40	153.80	16.25	255.78	1.43	16.07	0.85	3364.56
98	81.00	108.00	153.80	16.25	259.31	15.8	16.12	15.2	863.92
100	89.50	82.70	153.90	16.25	237.76	−2.59	15.77	−3.11	-1.26×10^{7}
102	89.30	84.70	153.90	16.25	240.03	24.6	15.81	24.1	202.97
104	88.00	86.10	154.00	16.25	240.15	463	15.81	462	-2.97×10^{13}
106	87.90	87.50	154.00	16.25	241.80	34.0	15.84	33.4	-2.21×10^{8}
108	89.00	88.70	154.00	16.25	244.71	19.2	15.89	18.6	611.04
110	90.70	90.70	154.00	16.25	249.40	11.9	15.97	11.3	1081.73
112	91.90	91.90	154.00	16.25	252.45	18.3	16.02	17.7	684.37
114	93.00	93.00	154.00	16.25	255.25	19.9	16.06	19.4	590.44
116	94.20	94.30	154.10	16.25	258.43	17.5	16.11	16.9	749.34
118	95.50	95.40	154.10	16.24	261.49	18.2	16.15	17.6	715.06
120	96.90	95.90	154.00	16.24	263.92	23.0	16.19	22.4	393.13
122	98.00	96.90	154.00	16.24	266.60	20.8	16.22	20.2	562.73
124	98.60	97.90	154.00	16.24	268.65	27.3	16.25	26.6	-2.06×10^{6}
126	99.10	98.90	154.00	16.24	270.57	29.0	16.27	28.4	-1.74×10^{7}
128	99.80	100.00	154.00	16.24	272.87	24.2	16.30	23.5	295.18
130	100.90	101.00	154.00	16.24	275.57	20.7	16.34	20.1	589.10
132	102.20	102.10	154.10	16.24	278.65	18.1	16.37	17.5	774.36
134	104.00	103.20	154.00	16.24	282.38	15.0	16.42	14.3	1002.42
136	104.70	104.30	154.10	16.23	284.70	24.1	16.45	23.4	325.09
138	105.30	105.50	154.00	16.23	287.01	24.0	16.47	23.3	332.92
140	106.10	106.50	154.00	16.23	289.34	24.0	16.50	23.3	339.02
142	106.90	107.50	154.00	16.23	291.66	24.0	16.52	23.3	345.08
142	108.60	108.60	154.00	16.23	295.28	0.0	16.56	−0.7	-5.7×10^{5}
144	110.50	109.70	154.10	16.23	299.16	14.4	16.60	13.6	1111.42
146	111.20	110.90	154.10	16.23	301.63	22.6	16.63	21.9	492.24
148	111.70	112.10	154.10	16.22	303.83	25.3	16.65	24.5	176.14

4.3 Results

The negative values in Table 2 and 3 for C_p, C_V and Θ_D are unphysical and are therefore not used in further calculations. The mean of all other calculated values for C_p, C_V and Θ_D result in

$$C_p = (25.74 \pm 0.29)\,\frac{\mathrm{J}}{\mathrm{mol\,K}} \tag{20}$$

$$C_V = (25.34 \pm 0.29)\,\frac{\mathrm{J}}{\mathrm{mol\,K}} \tag{21}$$

$$\Theta_D = 455.97\,\mathrm{K}. \tag{22}$$

5 Discussion

The measurement for the most part displays satisfactory results. The specific heat capacities show the expected relation $C_p - C_V > 0$ (see Section 2). The values for different temperatures are close to the spectrum shown in the literature, e. g. [5]. The mean of the experimentally determined values for Θ_D differ from the theoretical value $\Theta_{D\ \mathrm{Theory}}$ calculated in Equation 19 by 2.39 %. However, some measurements seem to be faulty, which can be seen in Figure 3 where prominent outliers are produced in the calculation of the specific heat capacities. Additionally, the method used to calculate the Debye temperature Θ_D seems to result in nonsensical negative values. The cause of this appears to be the interpolation; the full influence of which should be investigated further.

References

[1] TU Dortmund. *V47 Temperature dependence of molar heat of copper*. 2023.

[2] Thomas Prohaska et al. "Standard atomic weights of the elements 2021 (IUPAC Technical Report)". In: *Pure and Applied Chemistry* 94.5 (2022), pp. 573–600. DOI: doi:10.1515/pac-2019-0603. URL: https://doi.org/10.1515/pac-2019-0603.

[3] Kenneth Barbalace. *Periodic Table of Elements - Copper - Cu*. 1995 - 2024. URL: https://EnvironmentalChemistry.com/yogi/periodic/Cu.html (visited on 02/11/2024).

[4] Mark Winter. *The periodic table of the elements*. 1993-2024. (Visited on 02/15/2024).

[5] J. W. Arblaster. "Thermodynamic Properties of Copper". In: *Journal of Phase Equilibria and Diffusion* 36.5 (Oct. 2015), pp. 422–444. ISSN: 1863-7345. DOI: 10.1007/s11669-015-0399-x. URL: https://doi.org/10.1007/s11669-015-0399-x.